Theory of a Spherical Electrostatic Probe in a Continuum Gas: An Exact Solution

ERIC BAUM* AND ROBERT L. CHAPKIS*
TRW Systems Group, Redondo Beach, Calif.

The idealized problem of a spherical electrostatic probe in a quiescent continuum slightly ionized chemically frozen gas of uniform properties is treated. Exact solutions are obtained for the probe characteristic for the case of equal ion and electron temperatures over a wide range of probe potential and ratio of probe radius to Debye length. The results are compared with available approximate numerical solutions.

Nomenclature

$D_\pm$ = diffusion coefficient of positive or negative particles
e = absolute value of the charge on a charged particle
E^* = dimensionless electric field $= -(e\lambda_0/kT_-)d\phi/dr$
$J_\pm$ = normalized positive or negative particle flux $= -(\Gamma_\pm r)_p/D_\pm N_\infty$
J_T = dimensionless net charge flux $= -(\Gamma_{+p} - \Gamma_{-p})e^2r_p{}^3/\epsilon_0 kT_-D_+ = [(1 - K/\alpha)/(1 + K)]r_p{}^{*3}$
k = Boltzmann's constant
K = J_-/J_+
$N_\pm$ = local number density of positive or negative particles
r = radial distance measured from center of probe
s = normalized distance from probe $= (r - r_p)/\lambda_0$
$T_\pm$ = temperature of positive or negative particles
α = ratio of diffusion coefficients $= D_+/D_-$
$\beta_\pm$ = normalized number density of positive or negative particles $= (N_\pm/N_\infty)(\lambda_0/\lambda_D)^2$
$\Gamma_\pm$ = flux density (flux/unit area) of positive or negative particles
ϵ_0 = permittivity of empty space
λ_D = debye length $= (\epsilon_0 kT_-/N_\infty e^2)^{1/2}$
λ_0 = characteristic length $= [r_p\lambda_D{}^2/J_+(1 + K)]^{1/3}$
$\rho_p{}^2$ = dimensionless ambient positive or negative species concentration
= square of ratio of probe radius to debye length
$= N_\infty e^2r_p{}^2/\epsilon_0 kT_- = \beta_\infty r_p{}^{*2} = r_p{}^2/\lambda_D{}^2$
τ = ratio of positive-particle temperature to negative-particle temperature $= T_+/T_-$
ϕ = electrostatic probe potential
$\phi_p{}^*$ = dimensionless probe potential $= e\phi_p/kT_-$

Subscripts

p = conditions evaluated at the probe surface
∞ = conditions evaluated at $r \to \infty$

Introduction

THE current-voltage characteristic of an electrostatic probe is strongly dependent on the number density of charged particles in the surrounding gas. However, the usefulness of this probe as a diagnostic tool is limited, in the case of a collision dominated sheath, by the lack of an adequate theoretical model with which to relate the measured quantities to charge density. Cohen,[1] Su and Lam,[2] and more recently, Cicerone and Bowhill[3] investigated an idealized model of a probe in a quiescent plasma in which the principal assumptions are that; 1) continuum equations apply throughout, 2) the plasma is but slightly ionized, 3) all properties are spherically symmetric, 4) temperature is uniform (although an electron temperature distinct from the gas temperature is allowed), 5) no charged species' sources or sinks exist except at the probe surface, which is catalytic, and 6) the Einstein relation between mobility and diffusivity holds.

Solutions of the resulting equations were found by Cohen in the limit of debye length small compared to probe radius. Su and Lam and Cicerone and Bowhill found approximate solutions for the case of large bias potential. These investigators found it necessary to simplify the equations in order to make them more tractable, thereby introducing limitations on the range of validity of the solutions. Solutions to the complete equations were obtained over a limited range of Debye length to probe radius ratio and probe potential by Radbill,[4] using a method of quasi-linearization. In the present paper, exact solutions are presented for a wide range of bias potential and ratio of probe radius to debye length.

Received June 26, 1969; revision received November 17, 1969. The authors are indebted to M. Bilyk for writing the computer program that formed the basis of this work. They would like to express their appreciation for helpful discussions with G. Grohs, and especially with M. R. Denison, who suggested this problem. This work was performed for Bell Telephone Laboratories, Inc., Whippany, N. J. under Contract 6015-61, supported by the U.S. Army under Contract DAHC 60-69-C-0008.

* Member of the Technical Staff, Fluid Mechanics Laboratory. Member AIAA.

Equations

The equations governing the charged particle distribution and potential field about the spherical probe are the two continuity equations for the positive and negative particles and Poisson's equations relating the potential to the local charge density. For spherical symmetry these are

$$\begin{gathered}(d/dr)(r^2\Gamma_+) = 0\\ (d/dr)(r^2\Gamma_-) = 0 \\ (1/r^2)(d/dr)[r^2(d\phi/dr)] = (-e/\epsilon_0)(N_+ - N_-)\end{gathered} \tag{1}$$

The flux densities are related to the number densities and potential gradient by the following expression:

$$\Gamma_\pm = D_\pm[-dN_\pm/dr \mp (e/kT_\pm)N_\pm(d\phi/dr)] \tag{2}$$

In the previous expression we have assumed that the Einstein relation holds between the diffusion coefficients and the mobilities.

After integrating the first two of Eqs. (1) and combining with Eq. (2), we obtain the following:

$$(r^2/r_pN_\infty)[-dN_+/dr - (e/kT_+)N_+(d\phi/dr)] = -J_+ \tag{3}$$

$$(r^2/r_pN_\infty)[-dN_-/dr + (e/kT_-)N_-(d\phi/dr)] = -J_- \tag{4}$$

where the constants $J_\pm$ are the particle fluxes normalized by the diffusion particle fluxes received by the probe when it is at plasma potential, i.e.,

$$J_\pm = -(\Gamma_\pm r)_p/D_\pm N_\infty$$

At the probe surface $r = r_p$; $N_+ = N_- = 0$, $\Phi = \Phi_p$.

In the undisturbed plasma $r = \infty$; $\Phi = 0$. For given J_+ and J_- the potential Φ_p of the probe relative to the undisturbed plasma cannot be specified arbitrarily but is uniquely

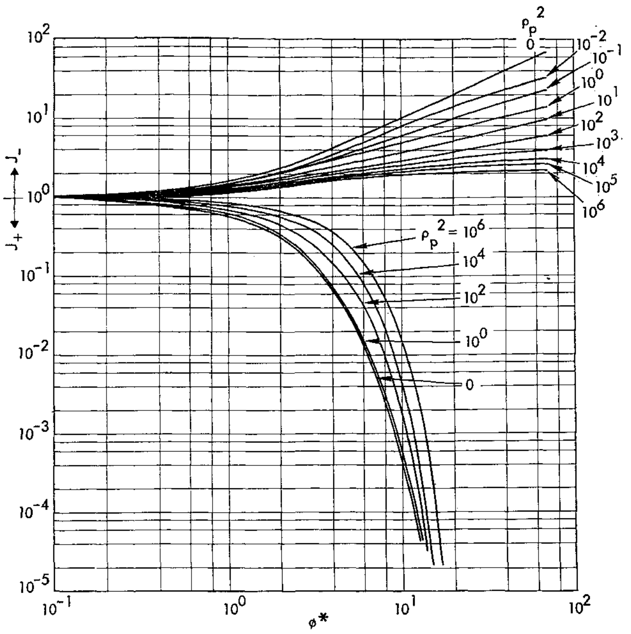

Fig. 1 Probe characteristics.

determined by the additional requirement that as $r \to \infty$; $N_+ \to N_\infty$, $N_- \to N_\infty$.

In order to put the equations into a form convenient for numerical integration, we first define two characteristic lengths

$$\lambda_D = \text{debye length} = [\epsilon_0 kT_-/N_\infty e^2]^{1/2}$$

$$\lambda_0 = [r_p\epsilon_0 kT_-/J_+(1+K)N_\infty e^2]^{1/3} = [r_p\lambda_D^2/J_+(1+K)]^{1/3}$$

where $K = J_-/J_+$.

We also define the following dimensionless dependent and independent variables:

$$E^* = -(e\lambda_0/kT_-)d\Phi/dr,\ \beta_+ = (N_+/N_\infty)(\lambda_0/\lambda_D)^2$$

$$\beta_- = (N_-/N_\infty)(\lambda_0/\lambda_D)^2,\ s = (r - r_p)/\lambda_0$$

The equations and boundary conditions then become

$$dE^*/ds + 2E^*/(r_p^* + s) = \beta_+ - \beta_-;\ E^*(0) = E_p^* \quad (5a)$$

$$1/(1+K) = (1 + s/r_p^*)^2[d\beta_+/ds - (1/\tau)\beta_+E^*] \quad \beta_+(0) = 0 \quad (5b)$$

$$K/(1+K) = (1 + s/r_p^*)^2(d\beta_-/ds + \beta_-E^*);\ \beta_-(0) = 0 \quad (5c)$$

where $r_p^* = r_p/\lambda_0$ and $\tau = T_+/T_-$ E_p^* is chosen to satisfy the quasineutrality condition

$$\beta_+(\infty) \to \beta_-(\infty) \to \beta_\infty \text{ as } s \to \infty$$

where $\beta_\infty = (\lambda_0/\lambda_D)^2$

Asymptotic Behavior

In order to solve these equations numerically, it is first necessary to know their asymptotic behavior far from the probe surface. The way in which the asymptotic solution is utilized is shown in the next section.

Far from the probe surface, one can represent the solutions of the equations in the form

$$E^* = \sum_{i=0} c_i(r_p^* + s)^{-i},\ \beta_+ = \sum_{i=0} a_i(r_p^* + s)^{-i}$$

$$\beta_- = \sum_{i=0} b_i(r_p^* + s)^{-i} \quad (6)$$

where the quasi-neutrality condition requires that $a_0 = b_0 = \beta_\infty$. Substitution into the equations yields the following recursion formulas:

$$c_{i+1} = -\frac{1}{(1+1/\tau)\beta_\infty}\left\{i(3-i)c_{i-1} + \sum_{j=2}^{i} c_j \times \left(\frac{a_{i-j+1}}{\tau} + b_{i-j+1}\right) + \delta_{1,i}\left(\frac{1-K}{1+K}\right) r_p^{*2}\right\} \quad (7)$$

$$a_i = \frac{1}{i}\left\{-\frac{1}{\tau}\sum_{j=2}^{i+1} c_j a_{i-j+1} - \frac{\delta_{1,i} r_p^{*2}}{1+K}\right\}$$

$$b_i = \frac{1}{i}\left\{\sum_{j=2}^{i+1} c_j b_{i-j+1} - \frac{\delta_{1,i} r_p^{*2} K}{1+K}\right\}$$

To examine the convergence of these series, it is convenient to write out several terms

$$E^* = \frac{-r_p^{*2}}{\beta_\infty(1+1/\tau)}\left(\frac{1-K}{1+K}\right)\frac{1}{(r_p^*+s)^2} \times \left\{1 - \frac{a_1}{\beta_\infty(r_p^*+s)} + \frac{a_1^2}{\beta_\infty^2(r_p^*+s)^2} - \frac{a_1^3}{\beta_\infty^3(r_p^*+s)^3} + \ldots - \left(\frac{4}{1+1/\tau}\right)\frac{a_1}{\beta_\infty^2}\frac{1}{(r_p^*+s)^3} + \left[\frac{10\tau a_1^2}{\beta_\infty^3(1+\tau)} + \frac{a_1}{\beta_\infty^3}\left(\frac{1-\tau}{1+\tau}\right)\frac{\tau r_p^{*2}}{(1+\tau)}\left(\frac{1-K}{1+K}\right)\right] \times \frac{1}{(r_p^*+s)^4}\cdots\right\} \quad (8)$$

$$\beta_+ = \beta_\infty + \frac{a_1}{(r_p^*+s)} + \frac{a_1^2}{\beta_\infty^2(1+\tau)} \times \left(\frac{1-K}{1+K/\tau}\right)\frac{1}{(r_p^*+s)^4} + \ldots$$

$$\beta_- = \beta_\infty + \frac{a_1}{(r_p^*+s)} - \frac{a_1^2}{\beta_\infty^2(1+\tau)} \times \left(\frac{1-K}{1+K/\tau}\right)\frac{1}{(r_p^*+s)^4} + \ldots$$

where

$$a_1 = \frac{-r_p^{*2}(\tau + K)}{(1+\tau)(1+K)}$$

For large r_p^*, the asymptotic behavior is reached at $s \ll r_p^*$ (thin sheath), where $\beta_+ \ll \beta_\infty$, so that

$$\beta_\infty \approx -a_1/r_p^*$$

$$|a_1/\beta_\infty(r_p^* + s)| \approx 1$$

The first group of terms in the series for E^* is very slowly convergent under these conditions. We can, however, sum

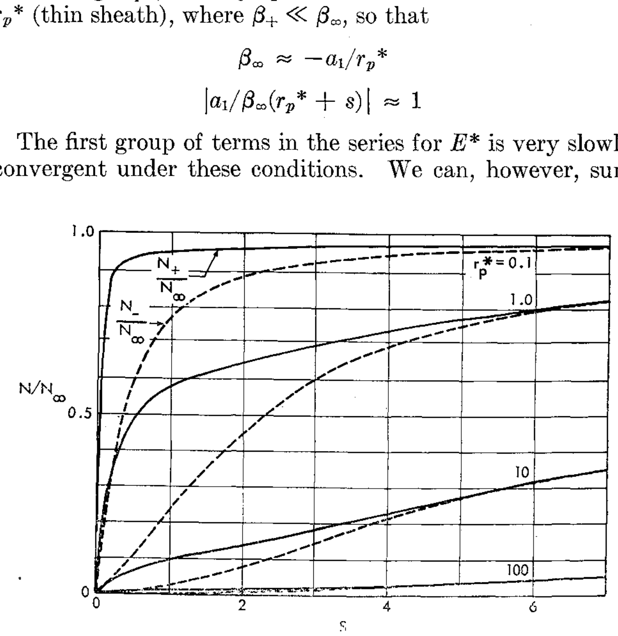

Fig. 2 $K = 0.05$: ion distribution.

Table 1 Probe characteristic data

r_p^*		$K = 10^{-30}$	10^{-20}	10^{-10}	10^{-5}	10^{-2}	2×10^{-2}	5×10^{-2}	10^{-1}	2×10^{-1}	5×10^{-1}	9×10^{-1}
1000	$\beta_\infty =$	491.54	493.58	496.05	497.66	498.98	499.15	499.40	499.59	499.77	499.95	499.99
	$-\Phi_p^* =$	77.04	53.88	30.61	18.82	11.32	10.41	8.993	7.633	5.878	2.791	0.4351
	$-E_p^* =$	5.9205	5.1371	4.0093	3.0813	2.0238	1.8435	1.5546	1.2848	0.95947	0.43984	0.067911
100		42.643	44.247	46.332	47.773	49.021	49.186	49.421	49.603	49.778	49.953	49.999
		74.68	51.43	28.28	16.51	9.073	8.207	6.917	5.758	4.353	2.029	0.3148
		6.4327	5.4779	4.1802	3.1675	2.0589	1.8734	1.5777	1.3026	0.97191	0.44521	0.068727
10		1.8480	2.2037	2.8529	3.4989	4.2615	4.3788	4.5508	4.6894	4.8251	4.9629	4.9991
		72.18	49.05	25.86	14.15	6.857	6.052	4.911	3.962	2.904	1.311	0.2019
		12.074	9.1783	5.9861	4.0578	2.4149	2.1762	1.8099	1.4814	1.0970	0.49918	0.076933
1		0.038295	0.051885	0.087102	0.14526	0.27555	0.30453	0.35170	0.39384	0.43829	0.48652	0.49967
		70.11	47.00	23.84	12.21	5.143	4.415	3.436	2.677	1.896	0.8274	0.1262
		73.408	49.814	25.982	13.828	6.2069	5.3855	4.2561	3.3555	2.4034	1.0604	0.16220
0.1		0.0016341	0.0024036	0.0046714	0.0091222	0.021774	0.025026	0.030605	0.035852	0.041626	0.048138	0.049955
		69.20	46.15	23.10	11.57	4.645	3.948	3.027	2.329	1.629	0.7024	0.1068
		693.61	462.90	232.02	116.42	46.893	39.891	30.616	23.577	16.511	7.1255	1.0836
0.01		0.00014556	0.00021812	0.00043562	0.00087028	0.0021303	0.0024577	0.0030217	0.0035545	0.0041430	0.0048091	0.0049953
		69.08	46.05	23.02	11.51	4.606	3.913	2.996	2.303	1.610	0.6934	0.1054
		6908.9	4606.1	2303.2	1151.7	460.82	391.48	299.81	230.45	161.09	69.383	10.546

this group of terms to get a form which is strongly convergent

$$1 - a_1/\beta_\infty(r_p^* + s) + a_1^2/\beta_\infty^2(r_p^* + s)^2 \ldots = (r_p^* + s)/(r_p^* + s + a_1/\beta_\infty)$$

The corresponding expression for the potential is then

$$\Phi^* = -\int_\infty^s E^* ds = \frac{-r_p^{*2}(1-K)}{\beta_\infty(1+K)(1+1/\tau)} \times \left\{\frac{\beta_\infty}{a_1} \ln\left(\frac{r_p^* + s + a_1/\beta_\infty}{r_p^* + s}\right) + \frac{1}{(1+1/\tau)} \times \frac{a_1}{\beta_\infty^2}\frac{1}{(r_p^*+s)^4} \cdots\right\} \quad (9)$$

Method of Solution

The set of Eqs. (5) has been solved numerically for the case of $\tau = 1$ over a range of values of r_p^* and K. The integration is started at the probe surface ($s = 0$) with an assumed value of E_p^*. An improper choice of E_p^* is recognized when either E^* or dE^*/ds changes sign, since the required solution has E^* going monotonically toward zero with increasing s. The method of regula falsi is used for converging on the proper value of E_p^*. An expression for β_∞ can be found using the asymptotic series to order $(r_p^* + s)^{-4}$, which for $\tau = 1$ gives

$$\beta_\infty = 1/2[\beta_+ + \beta_- + r_p^{*2}/(r_p^* + s)] \quad (10)$$

When $\beta_\infty(s)$ evaluated from this expression asymptotically approaches a constant with increasing s, the numerical and asymptotic solutions overlap.

The probe potential $\Phi_p^* = e\Phi_p/kT_-$ can then be found from

$$\Phi_p^* = -\int_\infty^0 E^* ds = -\int_\infty^s E^* ds + \int_0^s E^* ds \quad (11)$$

where the first integral is obtained from the asymptotic series to order $(r_p^* + s)^{-4}$. The number of significant figures required of E_p^* in order to extend the numerical solution into the asymptotic region can be as large as 12, depending on the values of r_p^* and K.

Results

Table 1 presents E_p^*, Φ_p^*, and β_∞ over a range of values of K and r_p^*. The parameters can be rearranged to give the following quantities of physical interest:

$$\rho_p^2 = N_\infty e^2 r_p^2/\epsilon_0 kT_- = \beta_\infty r_p^{*2} = r_p^2/\lambda_D^2$$

dimensionless ambient negative or positive species concentration;

$$J_+\rho_p^2 = -\Gamma_{+p}e^2 r_p^3/\epsilon_0 kT_- D_+ = r_p^{*3}/(1 + K)$$

dimensionless positive charged particle flux;

$$J_-\rho_p^2 = -\Gamma_{-p}e^2 r_p^3/\epsilon_0 kT_- D_- = r_p^{*3}K/(1 + K)$$

dimensionless negative charged particle flux;

$$J_T = -(\Gamma_{+p} - \Gamma_{-p})e^2 r_p^3/\epsilon_0 kT_- D_+ = [(1 - K/\alpha)/(1 + K)]r_p^{*3}$$

dimensionless net charge flux; where $\alpha = D_+/D_-$. Because of the symmetry of Eqs. (5) when $\tau = 1$, the results obtained for $K = a_1$, $E_p^* = a_2$, $\Phi_p^* = a_3$, $\beta_\infty = a_4$, and $r_p^* = a_5$ can be mapped into $K = 1/a_1$, $E_p^* = -a_2$, $\Phi_p^* = -a_3$, $\beta_\infty = a_4$, $r_p^* = a_5$.

The data of Table 1 were cross-plotted to obtain lines of constant ρ_p^2, and the resulting probe characteristics are shown in Fig. 1. The characteristics for $\Phi_p < 0$ can be obtained from this figure by letting $\Phi_p \to -\Phi_p$, $J_+ \to J_-$, $J_- \to J_+$. The characteristic for the limiting case $\rho_p \to 0$ was found using an asymptotic expansion evaluated to lowest order by Su and Lam and extended to include higher order terms in Ref. 5.

In the thin sheath limit ($\rho_p \to \infty$ or $r_p^* \to \infty$) $J_+ \to 2$ as $\Phi_p^* \to -\infty$. This can be easily shown from the asymptotic solution that gives $\beta_\infty \approx r_p^*/2$ for large r_p^*, since $J_+ = r_p^*/\beta_\infty(1 + K)$ and $K \to 0$ as $\Phi_p^* \to -\infty$. At a given finite value of Φ_p^*, however, it appears that $J_+ \to 1$ as $\rho_p \to \infty$. This is indicated by the asymptotic form of J_+ for $\rho_p \to \infty$ and $\Phi_p^* \to 0$ derived in Ref. 5 where it is shown that as $\rho_p \to \infty$, the slope of the curve of J_+ vs Φ_p^* approaches zero as $(\log \rho_p)^{-1}$.

The probe characteristics presented in Fig. 1 are probably the most useful results obtained from the integration of Eqs. (5). However, it is also interesting to see the detailed positive and negative particle distributions about the probe. These were obtained in the course of the numerical integration and are plotted in Figs. 2 and 3 for two values of K and for several values of r_p^*. Similar curves for the electric field are presented in Figs. 4 and 5. For the cases shown in Fig. 3, the

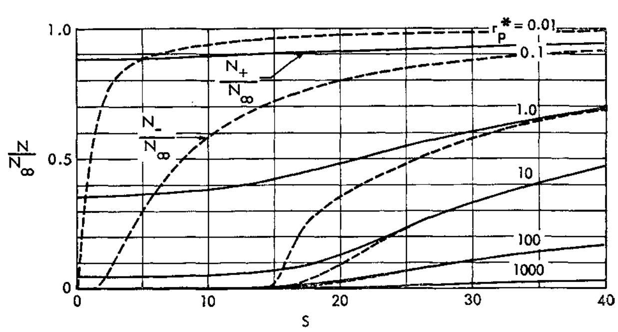

Fig. 3 $K = 10^{-30}$: **ion distribution.**

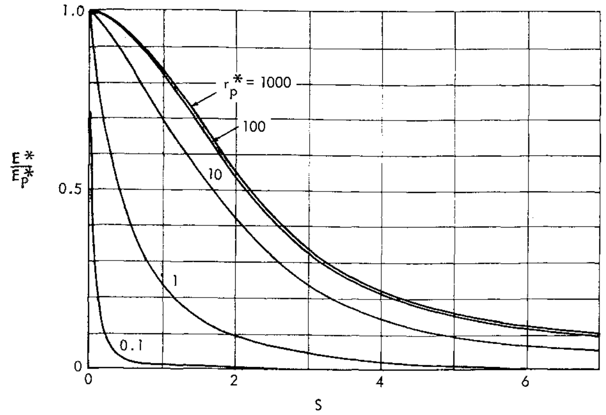

Fig. 4 $K = 0.05$: electric field.

ion concentration drops to zero rapidly in a region near the wall so thin that it is not visible on the scale of the graph.

It should be noted that the independent variable s used as the ordinate in Figs. 2–5 appears to be useful in that it enables one to present the results for a large range of $r_p{}^*$ and K on a single graph within a limited range of s. This is shown

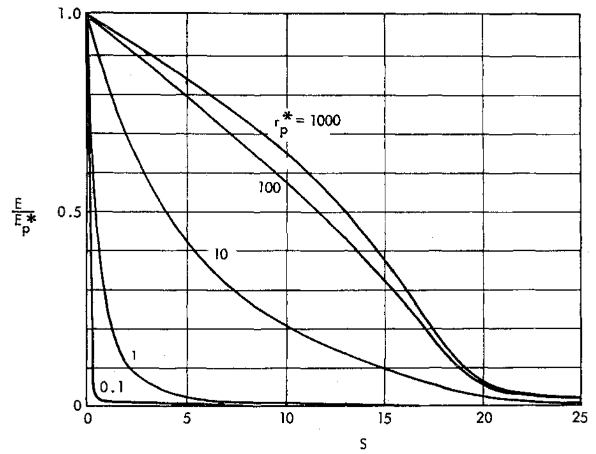

Fig. 5 $K = 10^{-30}$: electric field.

clearly in Fig. 6 which presents the sheath thickness [defined by the condition $2(\beta_i - \beta_e)/(\beta_i + \beta_e) = 0.01$] over the range of parameters in Table I. The ratio of sheath thickness to probe radius can be obtained directly from this figure since it is just $s/r_p{}^*$. Although the length λ_0 was introduced for computational convenience, it appears from these results that it is a measure of the sheath thickness.

The floating potential is of considerable interest and is found by imposing the condition $K = \alpha$. Figure 7 shows the

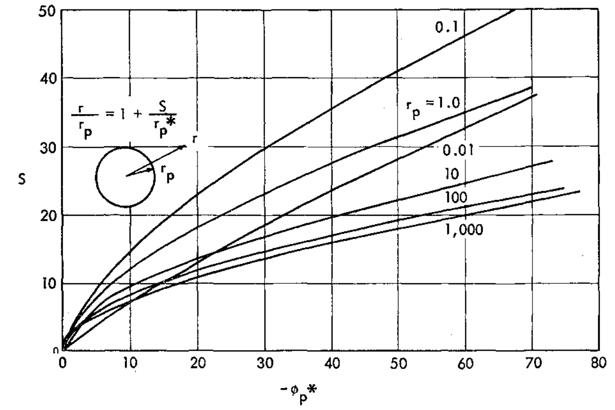

Fig. 6 Sheath thickness; sheath edge defined by $2(N_+ - N_-)/(N_+ + N_-) = 0.01$.

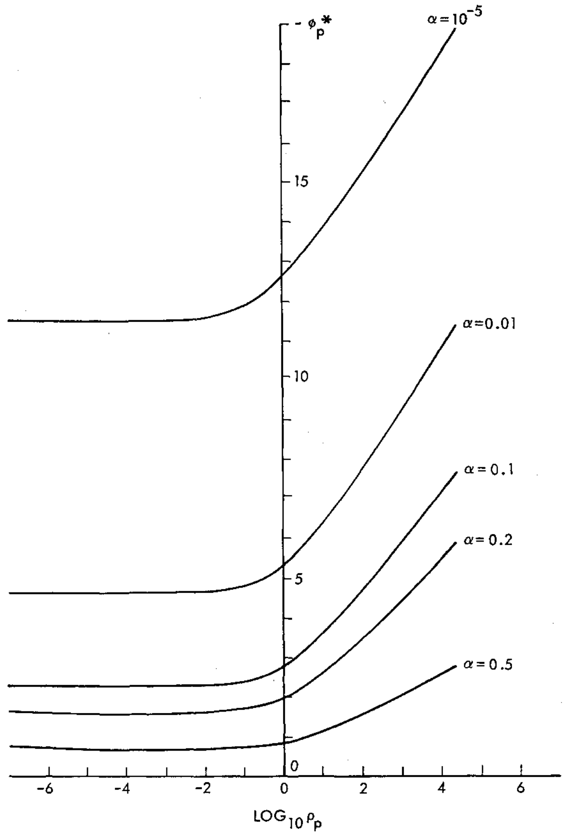

Fig. 7 Floating potential.

floating potential as a function of ρ_p for a range of values of α. The limiting value of $\Phi_p{}^*$ as $\rho_p \to 0$ agrees very well with the value predicted by the asymptotic expression of Su and Lam, $\Phi_p \to \ln K$.

Comparisons with Approximate Solutions

For large values of ρ_p, the probe characteristics obtained by Cohen agree well with those of Fig. 1. However, since Cohen's analysis is an asymptotic one valid for potential of order unity and thin sheath, the agreement becomes poorer with increasing $\Phi_p{}^*$ and decreasing ρ_p. In order to give some

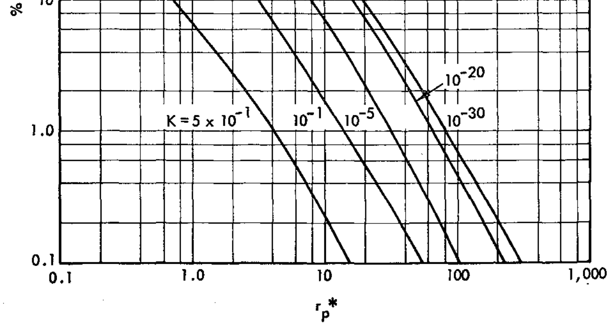

Fig. 8 Range of validity of Cohen's solution.

idea of the range of applicability of Cohen's solution, the percentage error in J_+ [from his Eq. (19)] as a function of r_p^* for constant values of K is given in Fig. 8.

Cicerone and Bowhill obtain numerical solutions for the attracted ion distribution at large probe potential and the corresponding probe characteristics. The characteristics presented, covering a range of $.1 < \rho_p < 1$ and an approximate potential range of $20 < \Phi_p^* < 500$, agree with the current results in the overlapping potential range, at least to within the accuracy attainable in reading the plotted data.

Conclusions

Numerical solutions of the spherical continuum electrostatic probe equations have been obtained for the case of equal electron and ion temperatures for a wide range of probe radius to Debye length ratio. Since the exact numerical solutions of the complete equations are straightforward and economical to obtain (in the range 15 to 25 seconds per solution on a CDC 6500 computer), it appears that further investigations of these equations should be aimed at finding simplified solutions of closed form. The numerical results presented here should prove valuable in assessing the accuracy of any such solutions.

References

[1] Cohen, I. M., "Asymptotic Theory of Spherical Electrostatic Probes in a Slightly Ionized, Collision-Dominated Gas," *Physics of Fluids*, Vol. 6, No. 10, Oct. 1963, pp. 1492–1499.

[2] Su, C. H. and Lam, S. H., "Continuum Theory of Spherical Electrostatic Probes," *Physics of Fluids*, Vol. 6, No. 10, Oct. 1963, pp. 1479–1491.

[3] Cicerone, R. J., and Bowhill, S. A., "Positive Ion Collection by a Spherical Probe in a Collision-Dominated Plasma," Rept. AR-21, 1967, Aeronomy Lab., Dept. of Electrical Engineering, Univ. of Illinois, Urbana, Ill.

[4] Radbill, J. R., "Computation of Electrostatic Probe Characteristics by Quasilinearization," *AIAA Journal*, Vol. 4, No. 7, July 1966, pp. 1195–1200.

[5] Baum, E. and Chapkis, R. L., "Theory of a Spherical Electrostatic Probe in a Continuum Gas: An Exact Solution," Rept. 06488-6242-R0-00, Dec. 1968, TRW Systems Group, Redondo Beach, Calif.

JUNE 1970 AIAA JOURNAL VOL. 8, NO. 6

Thin-Wire Langmuir-Probe Measurements in the Transition and Free-Molecular Flow Regimes

Michael G. Dunn* and John A. Lordi†
Cornell Aeronautical Laboratory Inc., Buffalo, N.Y.

Thin-wire Langmuir probes aligned with the flow direction have been used to measure the electron temperature and electron density in the inviscid nozzle flow of a short-duration reflected-shock tunnel. The electron density was inferred from the ion current portion of the probe characteristic and was simultaneously measured using microwave interferometers. The test gas used in these experiments was nitrogen at an equilibrium reservoir condition of 7200°K and 17.1 atm. At selected nozzle locations, the probe diameter and fineness ratio (L/D) of the probe were systematically varied in order to investigate probe performance in the transition and free-molecular flow regimes. The measured electron temperatures did not depend upon the probe diameter or the fineness ratio. The electron density inferred from the probe characteristic was found to be sensitive to collisional effects but insensitive to the fineness ratio in both the transition and free-molecular flow regimes. For free-molecular flow the results agree with Laframboise's theoretical predictions for ion collection in a portion of the orbital-motion-limited region. For probes having a radius less than a debye length in a free-molecular flow, the experimental results appear to disagree with the theory, the collected currents being larger than those predicted. In the transition-flow regime, the correction for collisional effects given by Talbot and Chou provides good agreement between the Langmuir-probe and microwave-interferometer electron-density data.

I. Introduction

THE behavior of thin-wire Langmuir probes in hypersonic flows is of interest because these probes provide a means for obtaining local measurements of electron temperature and electron density. Several authors[1–7] have demonstrated the utility of cylindrical probes in flow environments that are relatively well understood. However, even for such flow situations, there are still many aspects of electrostatic-probe operation that are not understood. Relatively few experiments have been reported in the literature that have systematically investigated the influence of various plasma and probe parameters on the electron density and electron temperatures deduced from the current-voltage characteristic. It is therefore the purpose of this paper to report the results of an experimental study that was undertaken in an effort to improve the understanding of thin-wire probes in hypersonic flows.

Several authors[8–12] have presented theoretical results for the current collected by thin-wire probes. Laframboise[8] has developed a numerical scheme for obtaining an iterative solution of the Bernstein and Rabinowitz[10] formulation. He presented tabulated results for the collected current for a wide range of probe potentials, ratios of probe radius to debye length, and ratios of ion temperature to electron temperature. These results have been used to interpret most of the

Received June 27, 1969; revision received December 22, 1969. This research was supported by NASA Goddard Space Flight Center, Greenbelt, Md., under Contract NAS 5-9978.

* Principal Engineer, Aerodynamic Research Department. Member AIAA.

† Research Aerodynamicist, Aerodynamic Research Department. Member AIAA.